Synthesis, structural characterization and biological evaluation of dinuclear gold(III) complexes with aromatic nitrogen-containing ligands: antimicrobial activity in relation to the complex nuclearity

Biljana Đ. Glišić,*[a] Nada D. Savić,[a] Beata Warżajtis,[b] Lidija Djokic,[c] Tatjana Ilic-Tomic,[c] Marija Antić,[a] Slavko Radenković,[a] Jasmina Nikodinovic-Runic,[c] Urszula Rychlewska[b] and Miloš I. Djuran[a]

[a]*Department of Chemistry, Faculty of Science, University of Kragujevac, R. Domanovića 12, PO Box 60, 34000 Kragujevac, Serbia*

[b] *Faculty of Chemistry, Adam Mickiewicz University, Umultowska 89B, 61-614 Poznań, Poland*

[c] *Institute of Molecular Genetics and Genetic Engineering, University of Belgrade, Vojvode Stepe 444a, 11000 Belgrade, Serbia*

*Corresponding author. Tel.: +381 34 300 251; fax: +381 34 335 040 (B. Đ. Glišić).

E-mail address: bglisic@kg.ac.rs (B. Đ. Glišić).

Abstract

Dinuclear gold(III) complexes {[$AuCl_3$]$_2$(μ-4,4'-bipy)} **(1)** and {[$AuCl_3$]$_2$(μ-bpe)} **(2)** with bridging aromatic nitrogen-containing heterocyclic ligands, 4,4'-bipyridine (4,4'-bipy) and 1,2-bis(4-pyridyl)ethane (bpe), were synthesized and characterized by NMR (^{1}H and ^{13}C), UV-vis and IR spectroscopic techniques. The crystal structure of **1** was determined by single-crystal X-ray diffraction analysis, while DFT M06-2X method was applied in order to optimize the structures of **1** and **2**. A detailed mechanistic study was performed using the same DFT approach in order to shed light on disparate coordination modes of the presently investigated N-heterocyclic ligands and the monocyclic pyrazine, which contains two nitrogen atoms within one ring, toward the $AuCl_3$ fragment. The investigation of the solution stability of **1** and **2** in DMSO revealed that both complexes were sufficiently stable in this solvent at room temperature. The complexes **1** and **2**, along with K[$AuCl_4$] and the N-heterocyclic ligands used for their synthesis, were evaluated by *in vitro* antimicrobial studies against a panel of the Gram-positive and Gram-negative bacteria and the fungus *Candida albicans*. In most cases, the complexes **1** and **2** have higher antibacterial activity than that of K[$AuCl_4$] (MICs for **1** and **2** were in the range 3.9-62.5 μg mL^{-1}), while both of the N-heterocycles did not affect the bacterial growth at concentrations up to 500 μg mL^{-1}. On the other hand, the antifungal activity of these two complexes against *C. albicans* was moderate and lower than that of K[$AuCl_4$]. In order to determine the therapeutic potential of **1** and **2**, their antiproliferative effect on the normal human lung fibroblast cell line MRC5 and embryotoxicity on zebrafish (*Danio rerio*) have also been evaluated. To the best of our knowledge, complexes **1** and **2** are the first examples of dinuclear gold(III) complexes with aromatic six-membered heterocycles containing two nitrogen atoms as bridging ligands.

Keywords: Gold(III) complexes; Structural characterization; DFT calculations; Antibacterial activity; Cytotoxicity; *Danio rerio*

TABLE OF CONTENTS

Crystal packing in 1

Packing of molecules of **1** in crystal is mostly governed by multiple C–H···Cl interactions and of which C1–H1···Cl2 at 1/2-*x*, -1/2-*y*, -*z* and C4–H4···Cl3 at 1/2-*x*, 1/2+*y*, 1/2-*z* are the shortest (2.72 and 2.71 Å, respectively). There are also several short C···Cl contacts around the C1 and C2 atoms; the distance Cl3(1/2-*x*, -1/2+*y*, 1/2-*z*)...C_g(C1-C2) is only 3.178(6) Å (C_g stands for the centre of gravity of the C1–C2 bond). According to the Hirshfeld surface analysis,[1] these two types of intermolecular interactions engage, respectively, 62.3 and 14.2% of the total molecular surface area. We could also identify relatively short Cl2...Cl2 (1-*x*, -*y*, -*z*) contact of 3.302(3) Å, shorter than the sum of the van der Waals radii (3.40 Å),[2] which most likely is sterically enforced, and a pair of interionic Au1...Cl1 (at 1/2-*x*, -1/2-*y*, -*z*) contacts of 3.673(2) Å around an inversion centre. Although these latter contacts are longer than the sum of the corresponding van der Waals radii (3.41 Å), they contribute to the extension of the coordination number of the Au(III) ion to 5 and to the formation of centrosymmetric dimers.

1 S. K. Wolff, D. J. Grimwood, J. J. McKinnon, M. J. Turner, D. Jayatilaka and M. A. Spackman, CrystalExplorer 3.5, University of Western Australia, Crawley, Australia, 2012.

2 A. Bondi, *J. Phys. Chem*., 1964, **68**, 441.

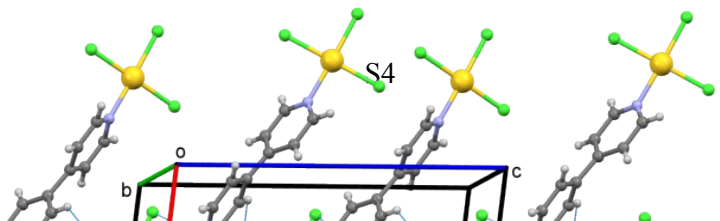

Fig. S1 Perspective view along the *b*-direction showing 3D supramolecular structure of **1**, stabilized by two most populated interactions; C–H···Cl (blue dashes) and C···Cl (beige dashes).

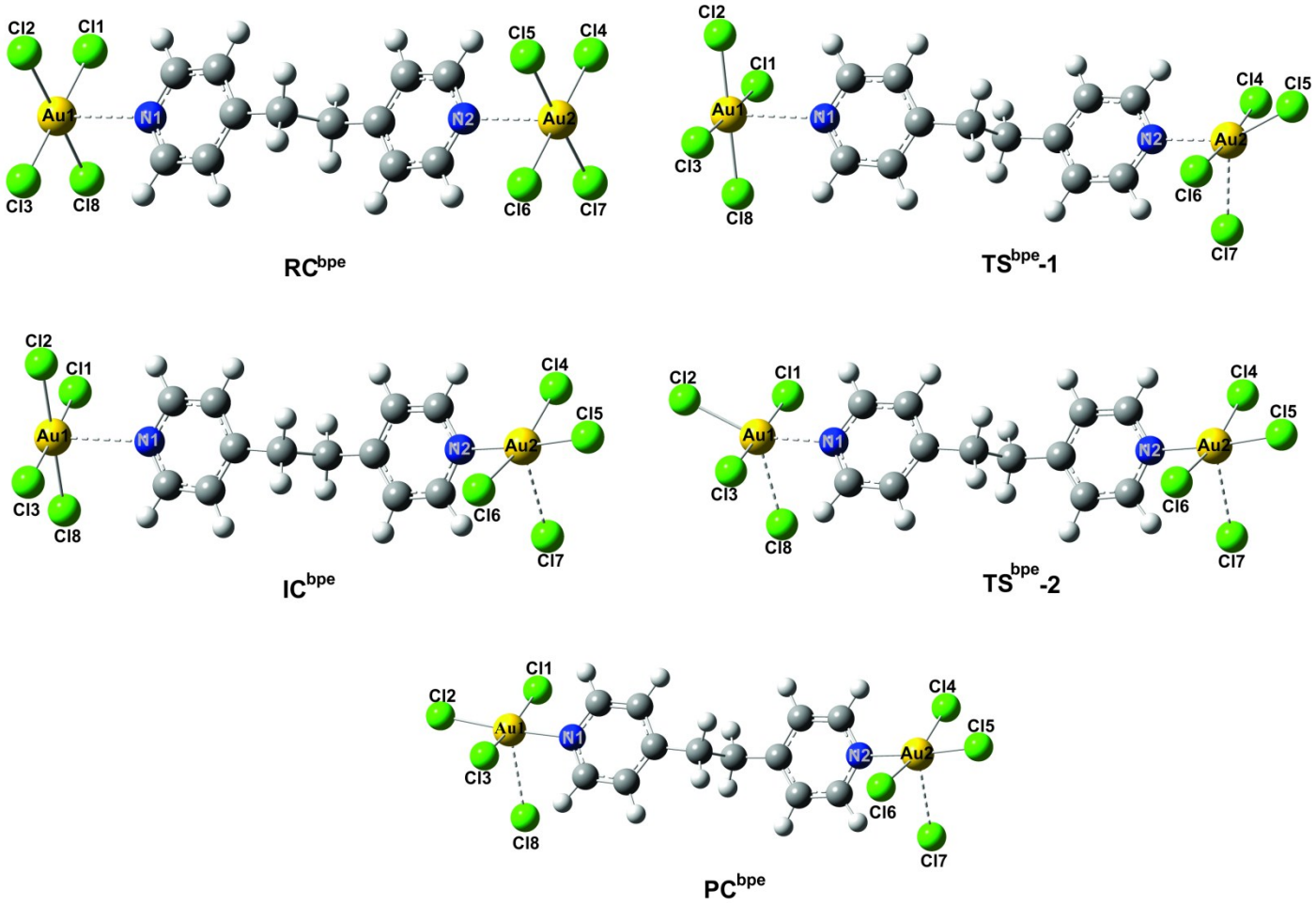

Fig. S2 Optimized geometries of the chemical species involved in the mechanism of formation of **2** obtained at the M06-2X/cc-PVTZ+LanL2TZ(f) level of theory.

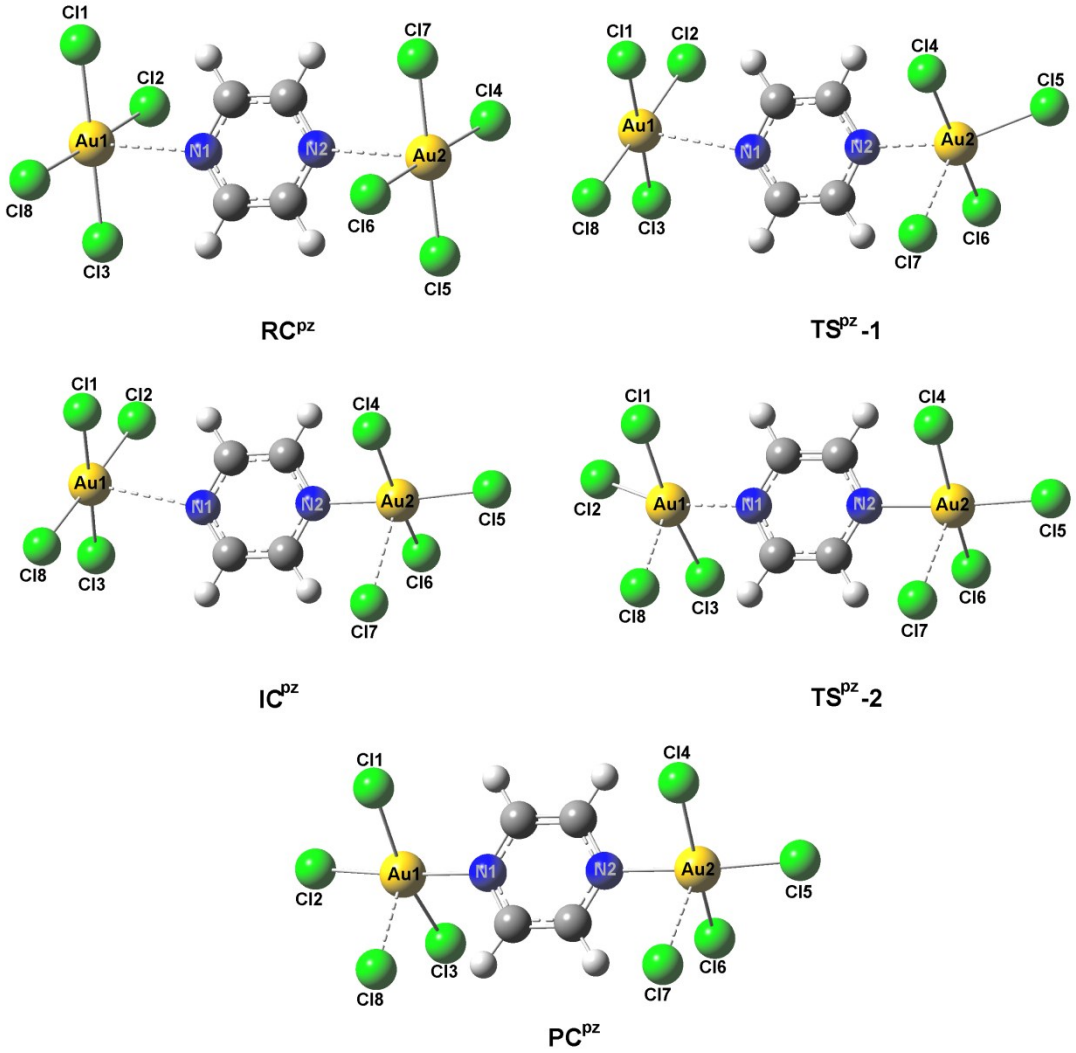

Fig. S3 The structures involved in the mechanism of the reaction of $[AuCl_4]^-$ with pz obtained at the M06-2X/cc-PVTZ+LanL2TZ(f) level of theory.

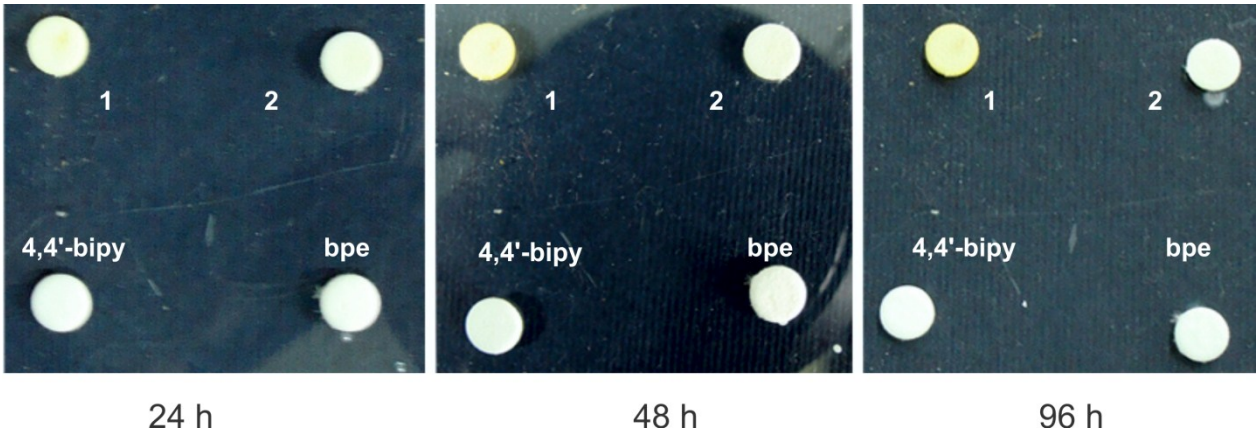

Fig. S4 Air/light stability of the DMSO solutions of dinuclear gold(III) complexes **1** and **2** and the corresponding N-heterocyclic ligands.

Table S1 Crucial interatomic distances (Å) in the structures involved in the mechanism of the reaction of $[AuCl_4]^-$ with 4,4'-bipy, bpe and pz calculated at the M06-2X/cc-PVTZ+LanL2TZ(f) level of theory

	Au1—N1	**Au1—Cl1**	**Au1—Cl2**	**Au1—Cl3**	**Au1—Cl8**	**Au2—N2**	**Au2—Cl4**	**Au2—Cl5**	**Au2—Cl6**	**Au2—Cl7**
RC^{bipy}	2.850	2.329	2.336	2.326	2.327	2.876	2.324	2.329	2.329	2.324
TS^{bipy}-1	2.872	2.328	2.328	2.324	2.323	2.310	2.311	2.325	2.317	2.725
IC^{bipy}	2.851	2.327	2.325	2.326	2.326	2.084	2.339	2.284	2.344	2.915
TS^{bipy}-2	2.300	2.315	2.319	2.314	2.736	2.084	2.339	2.284	2.344	2.915
PC^{bipy}	2.086	2.341	2.282	2.338	2.922	2.086	2.338	2.282	2.341	2.922
RC^{bpe}	2.843	2.326	2.326	2.326	2.324	2.844	2.326	2.324	2.326	2.326
TS^{bpe}-1	2.842	2.325	2.327	2.325	2.328	2.309	2.316	2.324	2.313	2.726
IC^{bpe}	2.849	2.323	2.328	2.327	2.325	2.083	2.343	2.283	2.337	2.930
TS^{bpe}-2	2.305	2.317	2.321	2.312	2.730	2.084	2.342	2.283	2.337	2.922
PC^{bpe}	2.084	2.342	2.283	2.338	2.925	2.084	2.342	2.283	2.337	2.920
RC^{pz}	2.903	2.328	2.325	2.324	2.326	2.904	2.326	2.328	2.325	2.324
TS^{pz}-1	2.961	2.327	2.327	2.321	2.320	2.309	2.315	2.329	2.312	2.725
IC^{pz}	2.971	2.326	2.329	2.320	2.318	2.083	2.341	2.288	2.337	2.924
TS^{pz}-2	2.265	2.322	2.314	2.310	2.757	2.098	2.347	2.282	2.337	2.870
PC^{pz}	2.104	2.348	2.280	2.336	2.863	2.104	2.348	2.280	2.336	2.862

Table S2 NBO charges (*e*) on Au, N and Cl for the structures involved in the mechanism of the reaction of $[AuCl_4]^-$ with 4,4'-bipy, bpe and pz calculated at the M06-2X/cc-PVTZ+LanL2TZ(f) level of theory

	q_{Au1}	q_{N1}	q_{C11}	q_{C12}	q_{C13}	q_{C18}	q_{Au2}	q_{N2}	q_{C14}	q_{C15}	q_{C16}	q_{C17}
RC^{bipy}	0.4643	-0.5120	-0.3790	-0.3794	-0.3786	-0.3781	0.4639	-0.5110	-0.3788	-0.3794	-0.3780	-0.3793
TS^{bipy}-1	0.4637	-0.5078	-0.3790	-0.3791	-0.3781	-0.3777	0.5143	-0.4939	-0.3431	-0.3394	-0.3526	-0.7286
IC^{bipy}	0.4636	-0.5042	-0.3791	-0.3784	-0.3783	-0.3795	0.5585	-0.4850	-0.3725	-0.3396	-0.3807	-0.8150
TS^{bipy}-2	0.5166	-0.4896	-0.3438	-0.3347	-0.3515	-0.7335	0.5585	-0.4827	-0.3796	-0.3377	-0.3727	-0.8126
PC^{bipy}	0.5580	-0.4813	-0.3782	-0.3362	-0.3720	-0.8121	0.5581	-0.4813	-0.3719	-0.3363	-0.3781	-0.8123
RC^{bpe}	0.4620	-0.5222	-0.3790	-0.3798	-0.3795	-0.3797	0.4620	-0.5221	-0.3795	-0.3797	-0.3790	-0.3798
TS^{bpe}-1	0.4616	-0.5214	-0.3799	-0.3796	-0.3796	-0.3789	0.5135	-0.4997	-0.3530	-0.3426	-0.3457	-0.7312
IC^{bpe}	0.4625	-0.5210	-0.3794	-0.3797	-0.3793	-0.3784	0.5597	-0.4897	-0.3822	-0.3442	-0.3736	-0.8180
TS^{bpe}-2	0.5141	-0.4986	-0.3453	-0.3411	-0.3538	-0.7332	0.5584	-0.4892	-0.3737	-0.3438	-0.3820	-0.8161
PC^{bpe}	0.5578	-0.4890	-0.3819	-0.3431	-0.3737	-0.8155	0.5587	-0.4889	-0.3813	-0.3421	-0.3743	-0.8161
RC^{pz}	0.5512	-0.4130	-0.3959	-0.3979	-0.3994	-0.3965	0.5520	-0.4130	-0.3965	-0.3960	-0.3979	-0.3994
TS^{pz}-1	0.5526	-0.3891	-0.3980	-0.3976	-0.3935	-0.3930	0.6111	-0.4140	-0.3660	-0.3480	-0.3578	-0.7623
IC^{pz}	0.5525	-0.3758	-0.3969	-0.3988	-0.3925	-0.3909	0.6481	-0.4051	-0.3923	-0.3461	-0.3860	-0.8471
TS^{pz}-2	0.6187	-0.3908	-0.3700	-0.3241	-0.3537	-0.7882	0.6401	-0.3929	-0.3922	-0.3253	-0.3796	-0.8363
PC^{pz}	0.6382	-0.3884	-0.3912	-0.3191	-0.3768	-0.8336	0.6381	-0.3883	-0.3912	-0.3191	-0.3769	-0.8335

Table S3 Effect percentages for abnormal morphological characteristics evaluated in the zebrafish teratogenicity assay (FET) at 96 hpf

Compound concentration	Dead embryos[a]	Teratogenic embryos[a]	Normal embryos[a]	Growth retardation[b]	Notochord[b]	Eyes[b]	Otoliths[b]	Pericardial edema[b]	Yolk edema[b]	Heart beat[b]	Blood circulation[b]	Unhatched[b]	Head malformation[c]	Skeletal deformities[c]
1														
50 µg/mL	90.00	10.00	0.00	0.00	0.00	0.00	0.00	0.00	0.00	0.00	0.00	100.00	*	*
40 µg/mL	30.00	70.00	0.00	0.00	0.00	0.00	0.00	0.00	0.00	0.00	0.00	100.00	*	*
30 µg/mL	10.00	90.00	0.00	0.00	0.00	0.00	0.00	0.00	0.00	0.00	0.00	100.00	*	*
20 µg/mL	0.00	46.67	53.33	0.00	0.00	0.00	0.00	0.00	0.00	0.00	0.00	53.33	0.00	0.00
10 µg/mL	0.00	0.00	100.00	0.00	0.00	0.00	0.00	0.00	0.00	0.00	0.00	0.00	0.00	0.00
5 µg/mL	0.00	0.00	100.00	0.00	0.00	0.00	0.00	0.00	0.00	0.00	0.00	0.00	0.00	0.00
4,4'-bipy														
50 µg/mL	100.00	0.00	0.00	-	-	-	-	-	-	-	-	-	-	-
40 µg/mL	100.00	0.00	0.00	-	-	-	-	-	-	-	-	-	-	-
30 µg/mL	100.00	0.00	0.00	-	-	-	-	-	-	-	-	-	-	-
20 µg/mL	80.00	20.00	0.00	100.00	0.00	0.00	0.00	100.00	100.00	0.00	100.00	66.67	100.00	100.00
10 µg/mL	0.00	0.00	100.00	0.00	0.00	0.00	0.00	0.00	0.00	0.00	0.00	0.00	0.00	0.00
5 µg/mL	0.00	0.00	100.00	0.00	0.00	0.00	0.00	0.00	0.00	0.00	0.00	0.00	0.00	0.00
2														
100 µg/mL	100.00	0.00	0.00	-	-	-	-	-	-	-	-	-	-	-
80 µg/mL	40.00	0.00	60.00	0.00	0.00	0.00	0.00	0.00	0.00	0.00	0.00	0.00	0.00	0.00
60 µg/mL	6.67	0.00	93.33	0.00	0.00	0.00	0.00	0.00	0.00	0.00	0.00	0.00	0.00	0.00
50 µg/mL	0.00	0.00	100.00	0.00	0.00	0.00	0.00	0.00	0.00	0.00	0.00	0.00	0.00	0.00
40 µg/mL	0.00	0.00	100.00	0.00	0.00	0.00	0.00	0.00	0.00	0.00	0.00	0.00	0.00	0.00
20 µg/mL	0.00	0.00	100.00	0.00	0.00	0.00	0.00	0.00	0.00	0.00	0.00	0.00	0.00	0.00
10 µg/mL	0.00	0.00	100.00	0.00	0.00	0.00	0.00	0.00	0.00	0.00	0.00	0.00	0.00	0.00
5 µg/mL	0.00	0.00	100.00	0.00	0.00	0.00	0.00	0.00	0.00	0.00	0.00	0.00	0.00	0.00
bpe														
100 µg/mL	10.00	90.00	0.00	100.00	0.00	0.00	0.00	100.00	0.00	0.00	0.00	0.00	0.00	88.89
80 µg/mL	0.00	100.00	0.00	100.00	0.00	0.00	0.00	100.00	0.00	0.00	0.00	0.00	0.00	73.33
60 µg/mL	0.00	60.00	40.00	60.00	0.00	0.00	0.00	60.00	0.00	0.00	0.00	0.00	0.00	60.00
50 µg/mL	0.00	30.00	70.00	30.00	0.00	0.00	0.00	30.00	0.00	0.00	0.00	0.00	0.00	0.00
40 µg/mL	0.00	20.00	80.00	0.00	0.00	0.00	0.00	20.00	0.00	0.00	0.00	0.00	0.00	0.00
20 µg/mL	0.00	0.00	100.00	0.00	0.00	0.00	0.00	0.00	0.00	0.00	0.00	0.00	0.00	0.00
10 µg/mL	0.00	0.00	100.00	0.00	0.00	0.00	0.00	0.00	0.00	0.00	0.00	0.00	0.00	0.00
5 µg/mL	0.00	0.00	100.00	0.00	0.00	0.00	0.00	0.00	0.00	0.00	0.00	0.00	0.00	0.00

Abrevitation used: (hpf) hours post fertilization; (-) data not available due to 100% mortality; (*) data not assessed because the embryos hatching has been prevented.; [a]Percentage of mortality based on all eggs; [b]Percentage of teratogenic effect based on all alive embryos at the time of assessment; [c]Percentage of teratogenic effect based on all alive hatched embryos at the time of assessment.

Table S4 Experimental details of **1**

Crystal data	
Chemical formula	$C_{10}H_8Au_2Cl_6N_2$
M_r	762.82
Crystal system, space group	Monoclinic, *C*2/*c*
Temperature (K)	130
a, *b*, *c* (Å)	16.2461 (6), 7.5152 (3), 14.1846 (5)
β (°)	97.938 (3)
V (Å^3)	1715.24 (11)
Z	4
Radiation type	Mo *K*α
μ (mm^{-1})	18.01
Crystal size (mm)	0.10 × 0.10 × 0.02
Data collection	
Diffractometer	Xcalibur
Absorption correction	Analytical
T_{min}, T_{max}	0.177, 0.574
No. of measured, independent and observed [$I > 2\sigma(I)$] reflections	12813, 1517, 1419
R_{int}	0.035
$(\sin \theta/\lambda)_{max}$ (Å^{-1})	0.595
Refinement	
$R[F^2> 2\sigma(F^2)]$, $wR(F^2)$, S	0.019, 0.049, 1.20
No. of reflections	1517
No. of parameters	91
H-atom treatment	H-atom parameters constrained
$\Delta\rho_{max}$, $\Delta\rho_{min}$ (e Å^{-3})	1.02, -0.45

Table S5 Lethal and teratogenic effects observed in zebrafish (*Danio rerio*) embryos at different hours post fertilization (hpf)

Category	Developmental endpoints	Exposure time (hpf)			
		24	48	72	96
Lethal effect	Egg coagulation[a]	•	•	•	•
	No somite formation	•	•	•	•
	Tail not detached	•	•	•	•
	No heartbeat		•	•	•
Teratogenic effect	Malformation of head	•	•	•	•
	Malformation of eyes[b]	•	•	•	•
	Malformation of sacculi/otoliths[c]	•	•	•	•
	Malformation of chorda	•	•	•	•
	Malformation of tail[d]	•	•	•	•
	Scoliosis	•	•	•	•
	Heartbeat frequency		•	•	•
	Blood circulation		•	•	•
	Pericardial edema	•	•	•	•
	Yolk edema	•	•	•	•
	Yolk deformation	•	•	•	•
	Growth retardation[e]	•	•	•	•

[a]No clear organs structure is recognized.
[b]Malformation of eyes was recorded for the retardation in eye development and abnormality in shape and size.
[c]Presence of no, one or more than two otoliths per sacculus, as well as reduction and enlargement of otoliths and/or sacculi (otic vesicles).
[d]Tail malformation was recorded when the tail was bent, twisted or shorter than to control embryos as assessed by optical comparation.
[e]Growth retardation was recorded by comparing with the control embryos in development or size (before hatching, at 24 hpf and 48 hpf) or in a body length (after hatching, at and onwards 72 hpf) by optical comparation using a inverted microscope (CKX41; Olympus, Tokyo, Japan).